Magnetic ground state and magnetic excitations in black dioptase $Cu_6Si_6O_{18}$

A. Podlesnyak,[1,*] O. Prokhnenko,[2] S. E. Nikitin,[3,4] A. I. Kolesnikov,[1] M. Matsuda,[1] S. E. Dissanayake,[1] T. R. Prisk,[5] H. Nojiri,[6] I. F. Díaz-Ortega,[6] M. K. Kidder,[7] and L. M. Anovitz[8]

[1]*Neutron Scattering Division, Oak Ridge National Laboratory, Oak Ridge, Tennessee 37831, USA*
[2]*Helmholtz-Zentrum Berlin für Materialien und Energie, D-14109 Berlin, Germany*
[3]*Max Planck Institute for Chemical Physics of Solids, Nöthnitzer Str. 40, D-01187 Dresden, Germany*
[4]*Institut für Festkörper- und Materialphysik, Technische Universität Dresden, D-01069 Dresden, Germany*
[5]*Center for Neutron Research, National Institute of Standards and Technology, Gaithersburg, Maryland 208996-6100, USA*
[6]*Institute for Materials Research, Tohoku University, Sendai, 980-8578, Japan*
[7]*Energy & Transportation Science Division, Oak Ridge National Laboratory, Oak Ridge, Tennessee 37831, USA*
[8]*Chemical Sciences Division, Oak Ridge National Laboratory, Oak Ridge, Tennessee 37831, USA*

(Received 4 June 2019; revised manuscript received 25 September 2019; published 1 November 2019)

The low-temperature magnetic properties and magnetic structure of fully dehydrated black dioptase $Cu_6Si_6O_{18}$ have been studied by single-crystal neutron diffraction and magnetization measurements in magnetic fields up to 30 T. The intrachain J_c and interchain J_{ab} interactions as well as the anisotropy of the exchange coupling J_c have been determined using inelastic neutron-scattering techniques. Zero-field antiferromagnetic order at $T_N = 6.7$ K can be described by a commensurate propagation vector of $\mathbf{k} = (0, 0, 3/2)$ with respect to the hexagonal $R\bar{3}$:H unit cell. The Cu magnetic moments are aligned antiferromagnetically along the c axis with about 12° tilt and are coupled ferromagnetically between the chains. The high-field magnetization measurements provide strong evidence for the presence of a spin-flop phase above 8 T. We found that J_c in black dioptase is significantly increased, while J_{ab} is much weaker compared to its counterpart, green dioptase $Cu_6[Si_6O_{18}]$ $6H_2O$. We suggest that black dioptase behaves like a nearly ideal $S = 1/2$ antiferromagnetic Heisenberg spiral chain with enhanced quantum fluctuations and weak spinon confinement $J_{ab}/J_c \sim 0.02$.

DOI: 10.1103/PhysRevB.100.184401

I. INTRODUCTION

Low-dimensional magnets have been one of the central subjects of condensed-matter physics due to the presence of significant quantum many-body effects such as dimensional crossover [1], fractionalized magnetic excitations (spinons) [2], condensation of magnetic excitations [3], and spin liquids [4]. One of the simplest quantum magnets is a spin-1/2 isotropic Heisenberg antiferromagnetic (AFM) 1D chain with a nearest-neighbor (NN) exchange interaction. This fundamental system has an exact analytic solution, the Bethe ansatz [5], and is currently well understood [6]. The magnetic dynamics of the 1D Heisenberg AFM chain are characterized by delocalized spinon excitations, which can be observed using inelastic neutron scattering (INS). The weak couplings between chains can lead to spinon confinement and form quantized spinon bound states [7,8]. The presence of such weak interchain exchange interactions tends to stabilize 3D long-range order and often creates a system with an exotic magnetic ground state. Recent studies of a growing number of newly synthesized 1D magnetic materials with interchain exchange open a world of fascinating magnetic phenomena and quantum phase transitions. Examples include spin-1/2 kagomè- and triangular-lattice Heisenberg antiferromagnets [9], spin ladders [10], and spin-Peierls transitions [11].

Besides laboratory-grown synthetic crystals, there are materials with complex magnetic structures created by nature [12] that show intriguing quantum phenomena. Although synthetic materials often have highly consistent properties with few unnecessary inclusions, many minerals are difficult to synthesize as single crystals large enough for experimental studies. This is especially true for the magnetic measurements using neutron-scattering techniques, which often require samples with a volume of several cubic millimeters. One example is a gem crystal green dioptase, known since ancient times and still attracting the attention of mineral collectors around the globe. The formal chemical composition of green dioptase was established in the 19th century as $Cu_6[Si_6O_{18}]$ $6H_2O$ [13]. Later it was found that the crystal structure consists of corrugated Si_6O_{18} rings interconnected by Cu^{2+} ions. Analogous rings of $6H_2O$ molecules alternate with the silicate rings along the c axis [14,15]. Each Cu^{2+} ion has two Cu NNs in a helical chain along the c axis and only one Cu in-plane neighbor forming a threefold spin-1/2 network (see Fig. 1). Magnetic susceptibility, specific heat, and neutron-diffraction measurements determined that green dioptase contains long-range AFM ordering at a Néel temperature $T_N \sim 14.5$ K and a reduced Cu-ordered magnetic moment $\sim 0.5\mu_B$ [16–18]. Our recent study of the magnetic interactions in green dioptase using INS found two important exchange interactions: NN AFM intrachain coupling $J_c = 10.6$ meV along the spiral chain and NN ferromagnetic (FM) interchain coupling $J_{ab} = -1.2$ meV, which forms Cu-dimers in the ab plane [19]. The small J_{ab}/J_c

*Corresponding author: podlesnyakaa@ornl.gov

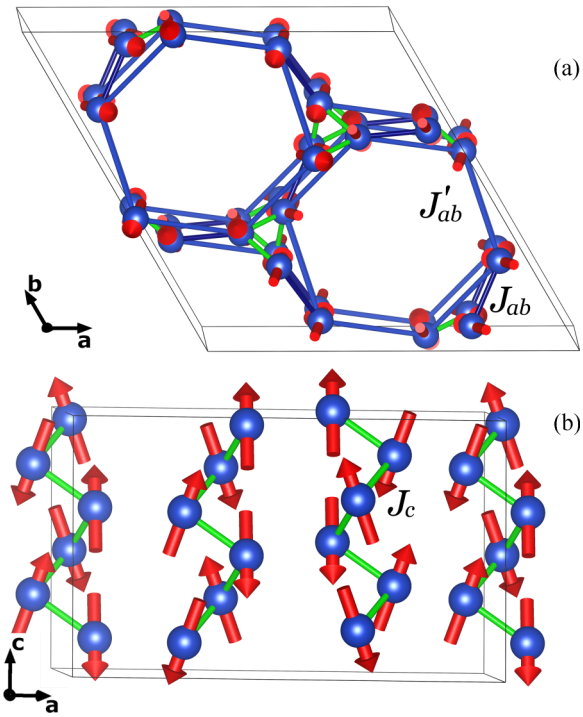

FIG. 1. Schematic crystal and magnetic structures of black dioptase showing the Cu atom positions only (blue spheres). (a) *ab* and (b) *ac* projection of part of the unit cell, showing the copper rings and the spiral copper chains, respectively. Both magnetic exchange interactions along the spiral chain (green) and interchain (blue) are indicated.

ratio puts green dioptase among the systems whose magnetic ground state features weekly coupled AFM spin-1/2 chains. A study of the effect of dehydration of $Cu_6[Si_6O_{18}]$ $6H_2O$ on the structural and magnetic properties by Law *et al.* [20] reveals that black dioptase is a one-dimensional AFM spin-1/2 Heisenberg quantum chain with a substantial intrachain exchange constant, which is about two orders of magnitude larger than exchange coupling between the chains.

Starting from natural green dioptase and following two different dehydration treatments, two different crystal structures can be synthesized. The first one, the orthorhombic polysilicate, $CuSiO_3$, has been a subject of intensive studies for the last 20 years due to its interesting magnetic properties and the possible presence of a spin-Peierls transition [21–26]. The second compound, completely dehydrated black dioptase $Cu_6Si_6O_{18}$, although known for more than a century [27], has been much less studied. The crystal structure of black dioptase keeps the 3D framework-type crystal structure of the parent green dioptase (see Fig. 1), but lacks water molecules [28]. The unit cell volume of $Cu_6Si_6O_{18}$ is reduced by about 2.4% compared to $Cu_6[Si_6O_{18}]$ $6H_2O$, which leads to considerable shortening of both in-chain and interchain Cu-Cu distances [15]. Because of this change, the strength of the magnetic interactions, governed by the superexchange between neighboring Cu^{2+} ions, is predicted to increase, and one should see markedly different magnetic properties relative to green dioptase.

Available information about the magnetic properties of $Cu_6Si_6O_{18}$ is limited. Little is known about magnetic excitations of this compound. The consensus is that black dioptase exhibits long-range AFM order similar to that described for green dioptase [16–18,20]. The estimated Néel temperature T_N for black dioptase ranges from 5 K [20] to 110 K [16] and the exchange interactions have only been evaluated from magnetic susceptibility measurements [20] and have never been confirmed by INS experiments. In this paper, we use neutron diffraction and INS, in combination with magnetization measurements in magnetic fields up to 30 T, to study the magnetic properties of black dioptase in detail.

II. EXPERIMENTAL DETAILS

Natural single crystals of green dioptase $Cu_6[Si_6O_{18}]$ $6H_2O$ were obtained commercially. The crystals were dehydrated by heating them in air at $T = 873$ K for 12 hours following the procedure described in Ref. [29]. The weight loss in the dehydrated sample showed that, within error, the water content had been reduced to zero by this process. The crystal structure and phase purity were examined by powder x-ray diffraction. The details of the sample characterization, including TGA and x-ray measurements, are in the Supplemental Material [30].

Bulk magnetic characterization of the sample was carried out by means of magnetic susceptibility and magnetization measurements up to 7 T at the Max Planck Institute, Dresden. High-field magnetization measurements were performed using a 30 T pulsed magnet and a ^{4}He flow cryostat at the Institute for Materials Research, Tohoku University (Sendai).

The magnetic structure of black dioptase was determined from neutron single-crystal integrated intensities obtained using the HB-1 triple-axis spectrometer installed at the High Flux Isotope Reactor (HFIR) at the Oak Ridge National Laboratory (ORNL). The fixed incident neutron energy was $E_i = 13.5$ meV ($\lambda = 2.46$ Å). The horizontal collimator sequence was $48' - 80' -$ sample $- 80' - 240'$. A pyrolytic graphite filter was placed after the sample to eliminate higher-order reflections.

The INS experiments were performed using two time-of-flight spectrometers: the fine-resolution Fermi chopper spectrometer SEQUOIA [31,32] and the Cold Neutron Chopper Spectrometer (CNCS) [33,34], both at the Spallation Neutron Source at ORNL. The data were collected from a single crystal with a mass of around 0.6 g, which was aligned in the $(H0L)$ scattering plane. The measurements were carried out using the rotating single crystal method at temperatures $T = 5.0$ K (SEQUOIA) and $T = 1.7$ K (CNCS). The incident neutron energy was fixed at $E_i = 65$ meV (SEQUOIA) and $E_i = 3.0$ meV (CNCS), resulting in a full width at half maximum energy resolution of 4.0 meV (SEQUOIA) and 0.07 meV (CNCS) at the elastic position.

The MANTID [35], HORACE [36], FULLPROF [37], BASIREPS [37], and VESTA [38] software packages were used for data reduction, analysis, and visualization. Linear spin-wave theory (LSWT), as realized in the SPINW program package [39], was used to calculate the excitation spectra and neutron scattering cross section of the spin Hamiltonian.

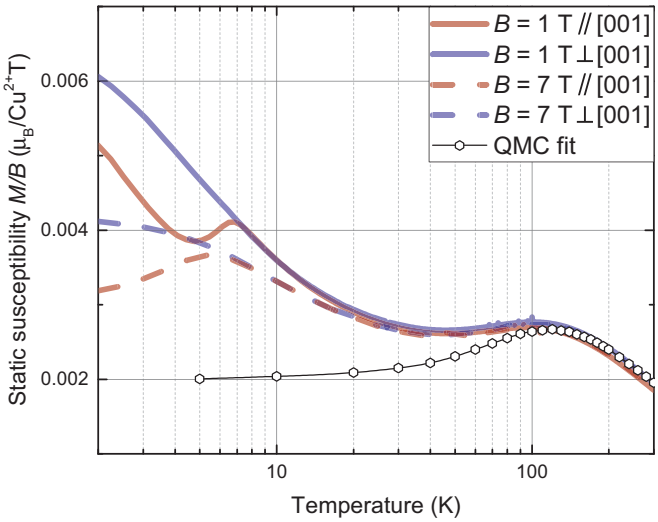

FIG. 2. Temperature dependencies of the static spin susceptibility of black dioptase measured at magnetic fields of 1 and 7 T applied parallel and perpendicular to the c axis ([001] direction) and the results of QMC calculations.

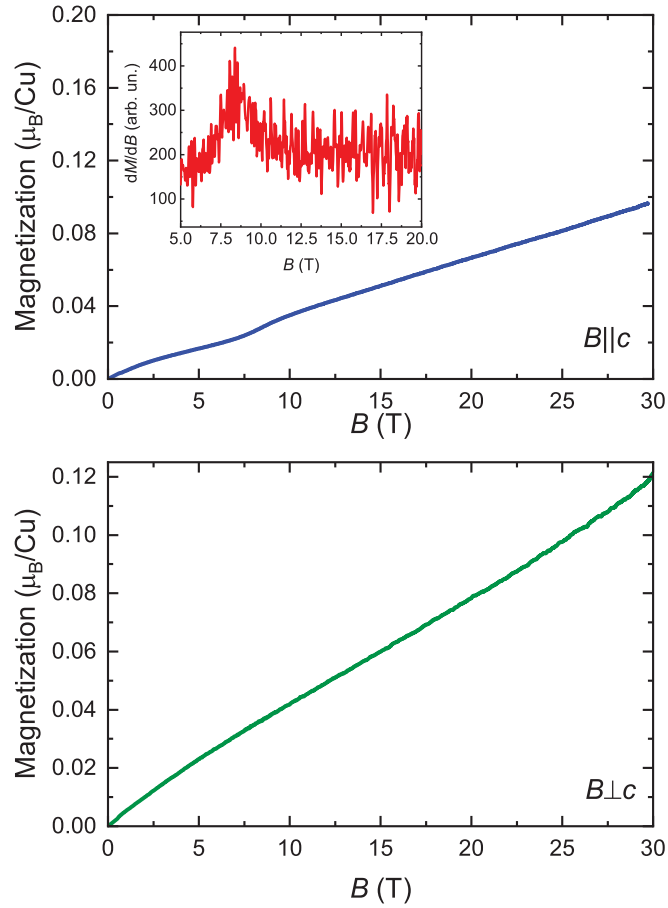

FIG. 3. Magnetization curves (solid line) of black dioptase at 1.5 K for a field applied parallel (top) and perpendicular (bottom) to the c axis. The inset shows a first derivative of the magnetization as a function of the magnetic field applied parallel to the c axis.

III. BULK PROPERTIES

Figure 2 shows the temperature dependencies of the static spin susceptibilities M/B measured at magnetic fields of 1 and 7 T applied both parallel and perpendicular to the c axis. First, let us consider the results obtained at $B = 1$ T. At high temperatures, both curves exhibit a broad maximum at $T^* \approx 100$ K, which can be associated with strong intrachain fluctuations [20]. When the magnetic field is applied along the c axis, a second peak appears at 6.7 K, whereas the curve measured with $B \perp c$ shows a monotonic increase down to the lowest available temperature (1.8 K). Such behavior indicates that the Cu^{2+} spins exhibit a transition to a long-range AFM state at $T_N = 6.7$ K, with the moments aligned parallel or close to parallel to the c axis. This value is close to the value of $T_N \sim 5$ K obtained from the specific-heat measurements [20]. On the other hand, the presence of magnetic impurities or defects induces a strong increase in magnetization at low temperatures for both geometries and hides the weak anomaly at T_N when $B \perp c$. A magnetic field of 7 T suppresses the impurity contribution (Curie-like tails) at low temperatures, but does not affect the high-temperature peak at T^*. Furthermore, the AFM ordering temperature shifts down to $T = 5.5$ K, as expected for a typical antiferromagnet. Thus, the magnetic behavior of black dioptase is dictated by two very different energy scales: strong intrachain coupling, which yields a peak at T^*, and a much weaker interchain interaction, which induces AFM ordering at T_N.

To quantitatively calculate the intrachain exchange interaction, we performed quantum Monte Carlo (QMC) modeling using the ALPS software package [40,41]. Simulations were performed on a chain of $N = 1000$ spins with $S = 1/2$ using the directed loop stochastic series expansion (SSE) application [42,43]. To reduce statistical errors, we used 150 000 sweeps for thermalization and 1 500 000 sweeps after thermalization in the temperature range $T/J = 0.03$–2. We calculated the magnetic susceptibility and tuned the intrachain exchange interaction J_c to fit the experimentally observed peak at T^* (see Fig. 2). This yielded an exchange interaction $J_c = 183$ K (15.77 meV). Our findings are in good agreement with those of Law *et al.* [20], who showed that the intrachain exchange is 174 K, and the interchain exchange is of the order of ~2 K.

Figure 3 displays the field dependence of the magnetization measured in a pulsed magnetic field up to 30 T applied parallel or perpendicular to the c axis. The absolute value of the magnetization was obtained by low-field measurements on a SQUID magnetometer. At both orientations, the magnetization grows almost linearly with field strength and does not show any saturation up to the highest field observed. For $B \perp c$, no anomalies were observed up to the maximum applied field. However, for $B \| c$ there is a metamagneticlike transition at about 8 T. A similar transition has been observed at 13 T in the parent green dioptase and attributed to a spin-flop transition [44]. In black dioptase, the transition appears at lower fields and the jump in magnetization is less pronounced. The inset in Fig. 3 shows a first derivative of the magnetization where the transition is more evident.

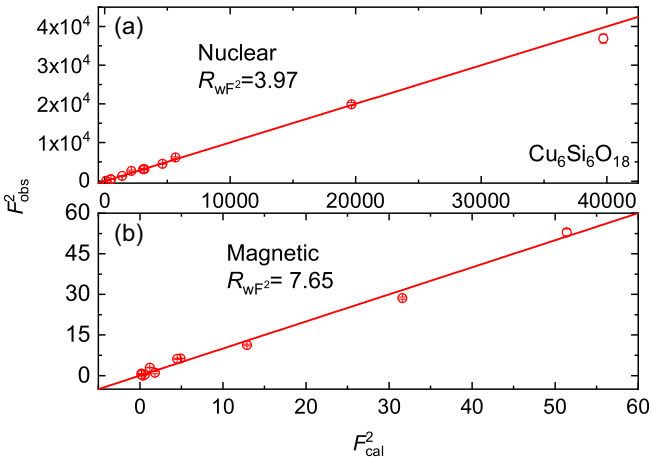

FIG. 4. Results of the refinement of nuclear (top) and magnetic (bottom) structures of black dioptaseat 4 K: Calculated vs observed intensities for the nuclear and magnetic peaks as obtained using FullProf. The straight line shows $F^2_{\rm obs} = F^2_{\rm calc}$. The reliability factors are also given.

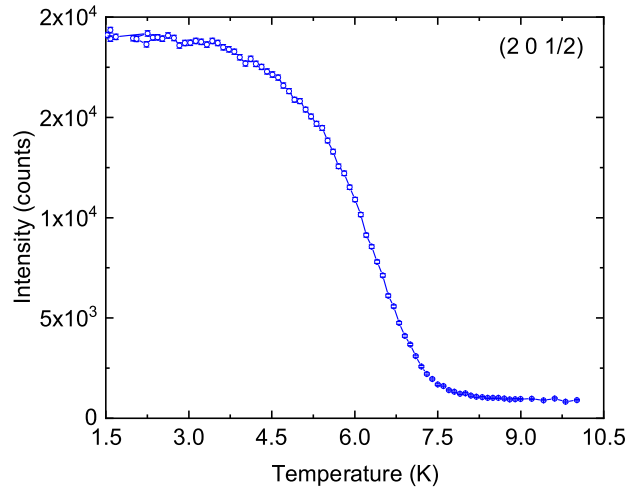

FIG. 5. Temperature dependence of the magnetic $(2, 0, 1/2)$ reflections as measured on the HB-1 spectrometer. Error bars throughout the text represent one standard deviation.

IV. MAGNETIC ORDER

Neutron-diffraction measurements for black dioptase, performed on a powder sample, were reported in Ref. [16]. The authors determined the propagation vector, $\mathbf{k}$=(0, 0, 1/2), and proposed a model where Cu magnetic moments of 0.5 μ_B are aligned along the c axis and coupled FM between the chains. Unfortunately, low intensities and a limited number of observed peaks precluded a proper magnetic structure refinement.

Here, we use single crystal neutron diffraction to determine the magnetic structure of black dioptase. The crystal was oriented on the HB-1 triple-axis spectrometer at HFIR such that the scattering plane was spanned by the vectors (1,0,0) and (0,0,1). Figure 4(a) shows the results of the nuclear refinement which has been performed to obtain the input parameters for the magnetic refinement. The good agreement between the observed and calculated intensities confirms that the crystal structure of black dioptasedoes not change upon cooling as expected. In addition to the nuclear reflections, a number of weak superlattice reflections were detected at temperatures below 8 K. The magnetic peaks can be indexed with a propagation vector $\mathbf{k} = (0, 0, 3/2)$ in the hexagonal cell, the same as was reported for the parent green dioptase [18]. Temperature dependence of the selected $(2, 0, 1/2)$ reflection, which is directly related to the magnetic order parameter, is shown in Fig. 5.

Using representational analysis, we determined the irreducible representations (irreps) (Table I) associated with little group $\mathbf{G_k}$, which contains all the symmetry elements leaving $\mathbf{k}$ invariant [37,45]. These irreps were used to define the possible magnetic structures which comply with all the symmetry operations of the little group $\mathbf{G_k}$. The best refinement using 11 nonequivalent magnetic reflections was then obtained for the magnetic structure associated with irrep Γ_2. This strongly resembles that of the parent compound [18]: The moments in the FM-coupled chains are aligned predominantly along the c axis with about 12° tilt. The Cu-moment is, however, further reduced as compared to the parent compound to 0.26(2) μ_B. The resulting magnetic structure is visualized in Fig. 1.

V. MAGNETIC EXCITATION SPECTRUM

Figures 6(a) and 6(c) show color contour plots of the magnetic excitation intensities $S(\mathbf{Q}, \omega)$ measured along the (0, 0, L) direction at temperatures below $T_{\rm N}$. The spin dynamics exhibit signs of quantum effects, i.e., a continuumlike spectrum with a magnon dispersing low-energy offset composed of two- and higher-order spinons [2]. The excitations are quite different from that found in green dioptase. First, the bandwidths of the magnetic excitations extend up to ∼30 meV compared to 12 meV in green dioptase [19]. Second, in contrast to the spectrum of $Cu_6[Si_6O_{18}]$ $6H_2O$, which comprises two distinct dispersive magnetic modes, we observe only the broad branch.

To check whether the minimum of the dispersion curve at the center of the magnetic Brillouin zone goes to zero energy, we obtained high-resolution INS spectra using the CNCS spectrometer. The spin excitation spectrum [Fig. 6(c)] reveals an energy gap of ∼1.8 meV at $(0, 0, 3/2)$, which confirms the presence of an easy axis anisotropy of the exchange interaction.

Contour maps of the scattering intensity in the (H, 0, L) plane integrated over the energy ranges $\hbar\omega = [6, 8]$ meV

TABLE I. Irreducible representation of the group $\mathbf{G_k}$ for the magnetic structure with $k = (0, 0, 3/2)$.

	1	3^+	3^-	$\bar{1}$	$\bar{3}^+$	$\bar{3}^-$
Γ_1	1	1	1	1	1	1
Γ_2	1	1	1	−1	−1	−1
Γ_3	1	$e^{\frac{2\pi i}{3}}$	$e^{\frac{4\pi i}{3}}$	1	$e^{\frac{2\pi i}{3}}$	$e^{\frac{4\pi i}{3}}$
Γ_4	1	$e^{\frac{2\pi i}{3}}$	$e^{\frac{4\pi i}{3}}$	−1	$e^{\frac{5\pi i}{3}}$	$e^{\frac{\pi i}{3}}$
Γ_5	1	$e^{\frac{4\pi i}{3}}$	$e^{\frac{2\pi i}{3}}$	1	$e^{\frac{4\pi i}{3}}$	$e^{\frac{2\pi i}{3}}$
Γ_6	1	$e^{\frac{4\pi i}{3}}$	$e^{\frac{2\pi i}{3}}$	−1	$e^{\frac{\pi i}{3}}$	$e^{\frac{5\pi i}{3}}$

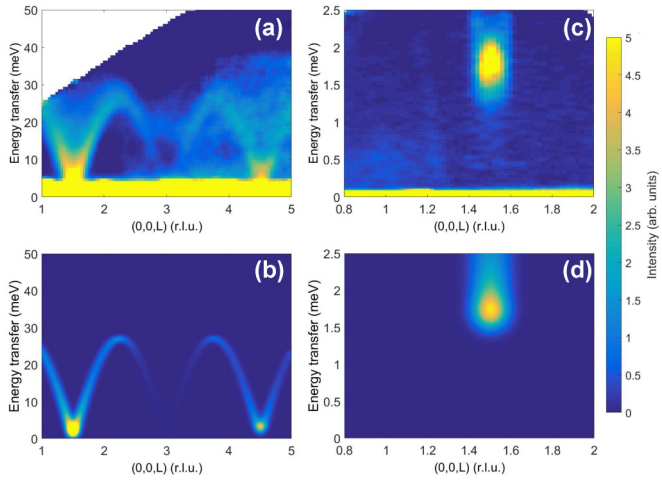

FIG. 6. Observed and simulated excitation spectra of black dioptase along the $(0, 0, \mathrm{L})$ direction measured at SEQUOIA (a), $T = 5.0$ K, and CNCS (c), $T = 1.7$ K. The integration along the H and K directions is ± 0.5 r.l.u. (b), (d) Simulation, based on the model cross section and the fitted parameter values, and convoluted with the spectrometer resolution, as described in the text. Note that r.l.u. stands for reciprocal lattice units. The intensity scale is the same in all panels and the data have been smoothed.

[Fig. 7(a)] and $\hbar\omega = [15, 17]$ meV [Fig. 7(c)] show rods of scattering that extend along the H direction. Similar behavior was observed for magnetic excitation along the K direction (not shown). Thus, within the resolution of our measurements, there is no dispersion along both H and K. This points to a very weak interchain coupling, which is evident in the one-dimensional behavior of the system.

It worth noting that, even though the magnetic excitations have no dispersion perpendicular to the L direction, their intensities change nonmonotonically with H. This behavior may arise as a consequence of the buckling of the magnetic chains, as discussed in detail in Ref. [46] and in the SM of Ref. [47]. Figure 1(b) shows a sketch of the crystal structure

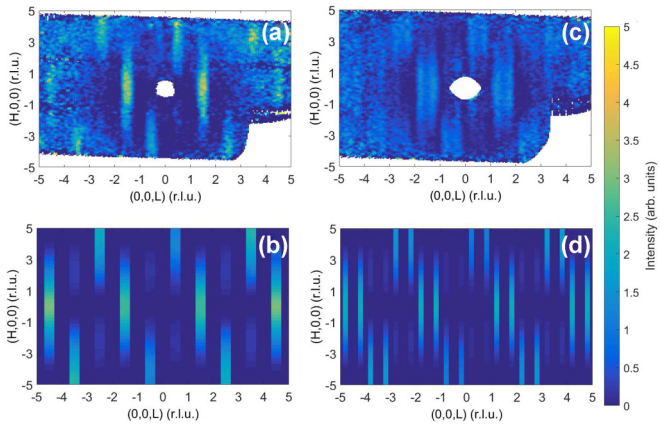

FIG. 7. Measured (top) and simulated (bottom) contour plots of the magnetic scattering of black dioptase in the $(H, 0, L)$ plane, integrated over the wave vector $K = [-0.5, 0.5]$ r.l.u., and the energy transfer $\hbar\omega = [6, 8]$ meV (a), (b) and $K = [-1.5, 1.5]$ r.l.u., $\hbar\omega = [15, 17]$ meV (c), (d).

and one can see that the Cu^{2+} ions form spirals, twisted along the c axis, rather than simple linear chains. Spin-wave calculations show that such a spiral structure does not change the dispersion curve but induces a redistribution of spectral intensity that correctly reproduces our experimental data, as can be seen in Fig. 7.

The spin Hamiltonian used for the spin-wave analysis of magnetic excitations in green dioptase [19] was

$$\mathcal{H} = \sum_{\langle i,j\rangle_c} \left(J_c \mathbf{S}_i \cdot \mathbf{S}_j + \Delta J_c S_i^z S_j^z\right) + \sum_{\langle i,j\rangle_{ab}} J_{ab} \mathbf{S}_i \cdot \mathbf{S}_j, \quad (1)$$

where J_{ab} and J_c are the interchain and intrachain exchange interactions, and the summations run over $\langle i, j\rangle_c$ and $\langle i, j\rangle_{ab}$ which denote bonds along the chains and bonds in the ab plane, respectively. Δ describes the anisotropy of the exchange coupling J_c. The corresponding labeling scheme is shown in Fig. 1. Our analysis closely follows that used in our previous work [19]. The standard least squares fitting procedure of the dispersion relations was used to get the best fit. For a direct comparison with the measured neutron intensities, the calculated spin-spin correlation function was convoluted with the instrumental resolution function. The intensities of the calculated spin waves were scaled to agree with the experiment. The agreement between the experimental and the calculated INS spectra nicely confirms the exchange parameters of Eq. (1), namely, $-0.5 < J_{ab} < 0$ meV, $J_c = 27.0(1)$ meV, and $\Delta J_c = 0.05(1)$ meV. However, the J_c value is significantly different from that obtained by fitting the magnetic susceptibility, which yields $J_c = 15.77$ meV. We discuss a possible origin of this disagreement below.

VI. DISCUSSION AND CONCLUSIONS

As confirmed by this study, both green and black dioptase are rare natural realizations of a magnetic model system useful for investigation of quasi-1D quantum magnetism. The final section of this paper will summarize our findings for black dioptase, and put the results in context of the recent magnetic studies of $Cu_6[Si_6O_{18}]\,6H_2O$ [19].

The results of the susceptibility and INS measurements show that the magnetic behavior of black dioptase is caused by a combination of intra (J_c) and interchain (J_{ab}) exchange interactions ($J_c \gg J_{ab}$), in which the anisotropy is relatively weak. In such a case, one can expect a strong effect of quantum fluctuations, which reduces an ordered moment. Refinement of the neutron-diffraction measurements shows that the ordered moment is indeed reduced almost four times down to 0.26(2) μ_B, compared to the full moment of 1 μ_B expected for Cu^{2+} ions. Furthermore, the elementary excitations of 1D $S = 1/2$ chains are fractionalized spinon quasiparticles, rather than classical magnons, and the excitation spectrum of the model is characterized by a broad continuum [2]. Indeed, such a continuum is clearly seen in the INS data presented in Fig. 6. However, our measurements were performed below T_N, where spinons get weakly confined and the majority of the spectral intensity is transferred to its lower boundary [7]. Note that the broadening of the INS spectrum due to site mixing, as was observed in some frustrated magnets, such as $YbMgGaO_4$ [48], is implausible in our case. Such Cu-Si mixing was not observed in the detailed single crystal structure study

of Belokoneva *et al.* [18] nor in our x-ray measurements, see the Supplemental Material. In addition, the continuum development in the quasi-1D $S = 1/2$ antiferromagnet is well known and expected (see, e.g., Ref. [49]). It also worth noting that the J_c value calculated by means of the LSWT exceeds that obtained by fitting the magnetic susceptibility with QMC by a factor of $J_c^{\mathrm{LSWT}}/J_c^{\mathrm{QMC}} = 1.71$, in full agreement with the classical result of des Cloizeaux and Pearson [50].

Comparing magnetic behavior of dehydrated black dioptase with that of its fully hydrated green counterpart, dehydration has a dual effect on the magnetic interactions: It significantly increases the intrachain exchange interaction J_c and simultaneously decouples the chains by suppressing J_{ab}. As a result, the results for black dioptase are much closer to the clean 1D Heisenberg limit. Consistently, despite the significant increase in J_c both the ordering temperature, T_{N}, of black dioptase and the ordered moment, m_{Cu}, are half as large as for those green dioptase. Furthermore, INS measurements of green dioptase can be correctly reproduced by means of LSWT, indicating that the spectra are dominated by conventional magnon excitations, whereas the continuum of excitations observed in black dioptase indicates the presence of fractionalized spinons.

ACKNOWLEDGMENTS

This research used resources at the High Flux Isotope Reactor and Spallation Neutron Source, a DOE Office of Science User Facility operated by the Oak Ridge National Laboratory. S.E.N. acknowledges support from the International Max Planck Research School for Chemistry and Physics of Quantum Materials (IMPRS-CPQM). O.P. acknowledges support by ICC-IMR, Tohoku University. This material is based upon work supported by the US Department of Energy, Office of Science, Office of Basic Energy Sciences, Chemical Sciences, Geosciences, and Biosciences Division. Powder x-ray diffraction measurements were conducted at the Center for Nanophase Materials Sciences (CNMS) (CNMS2019-R18) at the Oak Ridge National Laboratory (ORNL), which is a DOE Office of Science User Facility.

[1] B. Lake, D. A. Tennant, and S. E. Nagler, Novel Longitudinal Mode in the Coupled Quantum Chain Compound $KCuF_3$, Phys. Rev. Lett. **85**, 832 (2000).

[2] M. Mourigal, M. Enderle, A. Klöpperpieper, J.-S. Caux, A. Stunault, and H. M. Rønnow, Fractional spinon excitations in the quantum Heisenberg antiferromagnetic chain, Nat. Phys. **9**, 435 (2013).

[3] T. Giamarchi, C. Rüegg, and O. Tchernyshyov, Bose-einstein condensation in magnetic insulators, Nat. Phys. **4**, 198 (2008).

[4] L. Balents, Spin liquids in frustrated magnets, Nature **464**, 199 (2010).

[5] H. Bethe, Zur theorie der metalle, Z. Phys **71**, 205 (1931).

[6] A. Klümper, The spin-$\frac{1}{2}$ Heisenberg chain: Thermodynamics, quantum criticality and spin-Peierls exponents, Eur. Phys. J. B **5**, 677 (1998).

[7] A. K. Bera, B. Lake, F. H. L. Essler, L. Vanderstraeten, C. Hubig, U. Schollwöck, A. T. M. N. Islam, A. Schneidewind, and D. L. Quintero-Castro, Spinon confinement in a quasi-one-dimensional anisotropic Heisenberg magnet, Phys. Rev. B **96**, 054423 (2017).

[8] L. S. Wu, S. E. Nikitin, Z. Wang, W. Zhu, C. D. Batista, A. M. Tsvelik, A. M. Samarakoon, D. A. Tennant, M. Brando, L. Vasylechko, M. Frontzek, A. T. Savici, G. Sala, G. Ehlers, A. D. Christianson, M. D. Lumsden, and A. Podlesnyak, Tomonaga-Luttinger liquid behavior and spinon confinement in $YbAlO_3$, Nat. Commun. **10**, 698 (2019).

[9] S. Sachdev, Kagomè- and triangular-lattice Heisenberg antiferromagnets: Ordering from quantum fluctuations and quantum-disordered ground states with unconfined bosonic spinons, Phys. Rev. B **45**, 12377 (1992).

[10] E. Dagotto, Experiments on ladders reveal a complex interplay between a spin-gapped normal state and superconductivity, Rep. Prog. Phys. **62**, 1525 (1999).

[11] M. Hase, I. Terasaki, and K. Uchinokura, Observation of the Spin-Peierls Transition in Linear Cu^{2+} (Spin-$\frac{1}{2}$) Chains in an Inorganic Compound $CuGeO_3$, Phys. Rev. Lett. **70**, 3651 (1993).

[12] D. S. Inosov, Quantum magnetism in minerals, Adv. Phys. **67**, 149 (2018).

[13] H. Hess, Chemische analyse des dioptases, Ann. Phys. (Leipzig) **16**, 360 (1829).

[14] P. H. Ribbe, G. V. Gibbs, and M. M. Hamil, A refinement of the structure of dioptase, $Cu_6[Si_6O_{18}] \cdot 6H_2O$, Am. Mineral. **62**, 807 (1977).

[15] K.-H. Breuer, W. Eysel, and R. Müller, Structural and chemical varieties of dioptase, $Cu_6[Si_6O_{18}] \cdot 6H_2O$ II. Structural properties, Z. Kristallogr. Cryst. Mater. **187**, 15 (1989).

[16] M. Wintenberger, G. Andre, and M. F. Gardette, Magnetic properties of green dioptase $CuSiO_3H_2O$ and of black dioptase $CuSiO_3$, and magnetic structure of black dioptase, Solid State Commun. **87**, 309 (1993).

[17] I. A. Kiseleva, L. P. Ogorodova, L. V. Melchakova, and M. R. Bisengalieva, Thermodynamic properties of copper silicate: Dioptase: $Cu_6[Si_6O_{18}] \cdot 6H_2O$, J. Chem. Thermodynamics **25**, 621 (1993).

[18] E. L. Belokoneva, Yu. K. Gubina, J. B. Forsyth, and P. J. Brown, The charge-density distribution, its multipole refinement and the antiferromagnetic structure of dioptase, $Cu_6[Si_6O_{18}] \cdot 6H_2O$, Phys. Chem. Miner. **29**, 430 (2002).

[19] A. Podlesnyak, L. M. Anovitz, A. I. Kolesnikov, M. Matsuda, T. R. Prisk, S. Toth, and G. Ehlers, Coupled antiferromagnetic spin-$\frac{1}{2}$ chains in green dioptase $Cu_6[Si_6O_{18}]6H_2O$, Phys. Rev. B **93**, 064426 (2016).

[20] J. M. Law, C. Hoch, M.-H. Whangbo, and R. K. Kremer, Description of anhydrous (black) dioptase as a $S = 1/2$ uniform antiferromagnetic chain system, Z. Anorg. Allg. Chem. **636**, 54 (2010).

[21] H. H. Otto and M. Meibohm, Crystal structure of copper polysilicate, $Cu[SiO_3]$, Z. Kristallogr. **214**, 558 (1999).

[22] M. Baenitz, C. Geibel, M. Dischner, G. Sparn, F. Steglich, H. H. Otto, M. Meibohm, and A. A. Gippius, $CuSiO_3$: A quasi-one-dimensional $S = \frac{1}{2}$ antiferromagnetic chain system, Phys. Rev. B **62**, 12201 (2000).

[23] H. Wolfram, H. H. Otto, M. Cwik, M. Braden, G. André, F. Bourée, M. Baenitz, and F. Steglich, Neutron diffraction

study of the nuclear and magnetic structure of the quasi-one-dimensional compound $CuSiO_3$ around $T_N = 8$ K, Phys. Rev. B **69**, 144115 (2004).

[24] A. A. Gippius, A. S. Moskvin, M. Baenitz, S. L. Drechsler, E. N. Morozova, and H. H. Otto, $CuSiO_3$: A candidate system for purely oxygen antiferromagnet? Europhys. Lett. **63**, 282 (2003).

[25] H. Rosner, S.-L. Drechsler, K. Koepernik, R. Hayn, and H. Eschrig, Possibility of a spin-Peierls state in $CuSiO_3$ from electronic structure theory, Phys. Rev. B **63**, 073104 (2001).

[26] J. Sichelschmidt, M. Baenitz, C. Geibel, F. Steglich, A. Loidl, and H. H. Otto, Quasi-one-dimensional spin chains in $CuSiO_3$: an EPR study, Appl. Magn. Reson. **23**, 75 (2002).

[27] F. Zambonini, Investigations of some zeolite, Z. Kristallogr. **43**, 395 (1907).

[28] O. Janson, A. A. Tsirlin, M. Schmitt, and H. Rosner, Large quantum fluctuations in the strongly coupled spin-$\frac{1}{2}$ chains of green dioptase $Cu_6Si_6O_{18} \cdot 6H_2O$, Phys. Rev. B **82**, 014424 (2010).

[29] K.-H. Breuer and W. Eysel, Structural and chemical varieties of dioptase, $Cu_6[Si_6O_{18}] \cdot 6H_2O$ I. Thermal properties, Z. Kristallogr. Cryst. Mater. **184**, 1 (1988).

[30] See Supplemental Material at http://link.aps.org/supplemental/10.1103/PhysRevB.100.184401 for details of sample characterization.

[31] G. E. Granroth, A. I. Kolesnikov, T. E. Sherline, J. P. Clancy, K. A. Ross, J. P. C. Ruff, B. D. Gaulin, and S. E. Nagler, SEQUOIA: A newly operating chopper spectrometer at the SNS, J. Phys.: Conf. Ser. **251**, 012058 (2010).

[32] M. B. Stone, J. L. Niedziela, D. L. Abernathy, L. DeBeer-Schmitt, G. Ehlers, O. Garlea, G. E. Granroth, M. Graves-Brook, A. I. Kolesnikov, A. Podlesnyak, and B. Winn, A comparison of four direct geometry time-of-fight spectrometers at the Spallation Neutron Source, Rev. Sci. Instrum. **85**, 045113 (2014).

[33] G. Ehlers, A. Podlesnyak, J. L. Niedziela, E. B. Iverson, and P. E. Sokol, The new cold neutron chopper spectrometer at the spallation neutron source: Design and performance, Rev. Sci. Instrum. **82**, 085108 (2011).

[34] G. Ehlers, A. Podlesnyak, and A. I. Kolesnikov, The cold neutron chopper spectrometer at the Spallation Neutron Source: A review of the first 8 years of operation, Rev. Sci. Instrum. **87**, 093902 (2016).

[35] O. Arnold, J. C. Bilheux, J. M. Borreguero, A. Buts, S. I. Campbell, L. Chapon, M. Doucet, N. Draper, R. Ferraz Leal, M. A. Gigg, V. E. Lynch, A. Markvardsen, D. J. Mikkelson, R. L. Mikkelson, R. Miller, K. Palmen, P. Parker, G. Passos, T. G. Perring, P. F. Peterson, S. Ren, M. A. Reuter, A. T. Savici, J. W. Taylor, R. J. Taylor, R. Tolchenov, W. Zhou, and J. Zikovsky, Mantid–Data analysis and visualization package for neutron scattering and μSR experiments, Nucl. Instrum. Methods Phys. Res. Sect. A **764**, 156 (2014).

[36] R. A. Ewings, A. Buts, M. D. Le, J. van Duijn, I. Bustinduy, and T. G. Perring, HORACE: software for the analysis of data from single crystal spectroscopy experiments at time-of-flight neutron instruments, Nucl. Instrum. Methods Phys. Res. Sect. A **834**, 3132 (2016).

[37] J. Rodríguez-Carvajal, Recent advances in magnetic structure determination by neutron powder diffraction, Physica B: Condens. Matter **192**, 55 (1993).

[38] K. Momma and F. Izumi, *VESTA3* for three-dimensional visualization of crystal, volumetric and morphology data, J. Appl. Cryst. **44**, 1272 (2011).

[39] S. Toth and B. Lake, Linear spin wave theory for single-Q incommensurate magnetic structures, J. Phys.: Condens. Matter **27**, 166002 (2015).

[40] B. Bauer, L. D. Carr, H. G. Evertz, A. Feiguin, J. Freire, S. Fuchs, L. Gamper, J. Gukelberger, E. Gull, S. Guertler, A. Hehn, R. Igarashi, S. V. Isakov, D Koop, P. N. Ma, P. Mates, H. Matsuo, O. Parcollet, G Pawłowski, J. D. Picon, L. Pollet, E. Santos, V. W. Scarola, U. Schollwöck, C. Silva, B. Surer, S. Todo, S Trebst, M. Troyer, M. L. Wall, P. Werner, and S. Wessel, The ALPS project release 2.0: open source software for strongly correlated systems, J. Stat. Mech. Theory Exp. (2011) P05001.

[41] A. F. Albuquerque, F. Alet, P. Corboz, P. Dayal, A. Feiguin, S. Fuchs, L. Gamper, E. Gull, S. Gürtler, A. Honecker, R. Igarashi, M. Körner, A. Kozhevnikov, A. Läuchli, S. R. Manmana, M. Matsumoto, I. P. McCulloch, F. Michel, R. M. Noack, G. Pawłowski, L. Pollet, T. Pruschke, U. Schollwöck, S. Todo, S. Trebst, M. Troyer, P. Werner, and S. Wessel, The ALPS project release 1.3: Open-source software for strongly correlated systems, J. Magn. Magn. Mater. **310**, 1187 (2007).

[42] A. W. Sandvik, Stochastic series expansion method with operator-loop update, Phys. Rev. B **59**, R14157 (1999).

[43] F. Alet, S. Wessel, and M. Troyer, Generalized directed loop method for quantum monte carlo simulations, Phys. Rev. E **71**, 036706 (2005).

[44] H. Ohta, M. Fujisawa, N. Souda, S. Okubo, E. Ohmichi, T. Sakurai, H. Kikuchi, T. Ono, H. Tanaka, K. Matsubayashi, and Y. Uwatoko, Magnetic susceptibility measurement under high pressure and magnetization measurement of $S = 1/2$ dioptase lattice antiferromagnet, J. Phys.: Conf. Ser. **150**, 042151 (2009).

[45] E. F. Bertaut, Representation analysis of magnetic structures, Acta Cryst. **A24**, 217 (1968).

[46] I. Cabrera, J. D. Thompson, R. Coldea, D. Prabhakaran, R. I. Bewley, T. Guidi, J. A. Rodriguez-Rivera, and C. Stock, Excitations in the quantum paramagnetic phase of the quasi-one-dimensional Ising magnet $CoNb_2O_6$ in a transverse field: Geometric frustration and quantum renormalization effects, Phys. Rev. B **90**, 014418 (2014).

[47] S. E. Nikitin, L. S. Wu, A. S. Sefat, K. A. Shaykhutdinov, Z. Lu, S. Meng, E. V. Pomjakushina, K. Conder, G. Ehlers, M. D. Lumsden, A. I. Kolesnikov, S. Barilo, S. A. Guretskii, D. S. Inosov, and A. Podlesnyak, Decoupled spin dynamics in the rare-earth orthoferrite $YbFeO_3$: Evolution of magnetic excitations through the spin-reorientation transition, Phys. Rev. B **98**, 064424 (2018).

[48] Y. Li, D. Adroja, R. I. Bewley, D. Voneshen, A. A. Tsirlin, P. Gegenwart, and Q. Zhang, Crystalline Electric-Field Randomness in the Triangular Lattice Spin-Liquid $YbMgGaO_4$, Phys. Rev. Lett. **118**, 107202 (2017).

[49] A. Zheludev, M. Kenzelmann, S. Raymond, E. Ressouche, T. Masuda, K. Kakurai, S. Maslov, I. Tsukada, K. Uchinokura, and A. Wildes, Energy Separation of Single-Particle and Continuum States in an $S = 1/2$ Weakly Coupled Chains Antiferromagnet, Phys. Rev. Lett. **85**, 4799 (2000).

[50] J. Des Cloizeaux and J. J. Pearson, Spin-wave spectrum of the antiferromagnetic linear chain, Phys. Rev. **128**, 2131 (1962).